Journal of Computational Physics **173,** 149–174 (2001)
doi:10.1006/jcph.2001.6864, available online at http://www.idealibrary.com on IDEAL®

High-Order Finite Difference Methods, Multidimensional Linear Problems, and Curvilinear Coordinates

Jan Nordström* and Mark H. Carpenter†

*Computational Aerodynamics Department, Aerodynamics Division (FFA), The Swedish Defense Research Agency (FOI) and the Department of Scientific Computing, Information Technology, Uppsala University, Uppsala, Sweden; and †Computational Modeling and Simulation Branch, NASA Langley Research Center, Hampton, Virginia 23681
E-mail: jan.nordstrom@foi.se; m.h.carpenter@larc.nasa.qov

Received February 21, 2000; revised April 23, 2001

Boundary and interface conditions are derived for high-order finite difference methods applied to multidimensional linear problems in curvilinear coordinates. Difficulties presented by the combination of multiple dimensions and varying coefficients are analyzed. In particular, problems related to nondiagonal norms, a varying Jacobian, and varying and vanishing wave speeds are considered. The boundary and interface conditions lead to conservative schemes and strict and strong stability provided that certain metric conditions are met.

1. BACKGROUND

Phenomena that require an accurate description of high-frequency variation in space for long times occur in many important applications such as electromagnetics, acoustics (all cases of wave propagation), and direct simulation of turbulent and transitional flow; see, for example [1–6]. Strictly stable high-order finite difference methods are well suited for these types of problems (see [7–16]) because they guarantee bounded error growth in time for realistic meshes.

Most of the development for these types of methods has considered constant-coefficient problems on a Cartesian mesh. In [17] and [18], stable and conservative boundary and interface conditions were derived for the one-dimensional (1D) constant coefficient Euler and Navier–Stokes equations on multiple domains. A similar technique was used in [19–21] for Chebyshev spectral methods.

In this paper we extend the constant-coefficient analyzis in [17] and [18] to scalar multidimensional linear problems in curvilinear coordinates including block interfaces. Related

0021-9991/01 $35.00

previous work includes investigations of the metric derivatives in nonsmooth meshes (see [22, 23]) and the treatment of parabolic and hyperbolic systems in curvilinear coordinates on a single domain [14]. Many of the issues discussed in this paper are adressed in [24].

The rest of this paper will proceed as follows. Section 2 introduces the problem. Section 3 defines the continuous problem and discusses well-posedness. Section 4 provides an investigation of the discrete problem. Section 5 illustrates numerical experiments and in Section 6 we summarize and draw conclusions.

2. INTRODUCTION

The 2D linear problem considered in this paper is

$$\begin{aligned} u_t + F_x + G_y &= h, \quad [x, y] \in \Omega, \quad t \geq 0, \\ u &= f, \quad [x, y] \in \Omega, \quad t = 0, \\ Lu &= g, \quad [x, y] \in \delta\Omega, \quad t \geq 0, \end{aligned} \tag{1}$$

where h, f, g are the data of the problem, L is the boundary operator, and

$$\begin{aligned} F &= F^I + F^V, \quad F^I = a_1 u, \quad F^V = -(b_{11}u_x + b_{12}u_y), \\ G &= G^I + G^V, \quad G^I = a_2 u, \quad G^V = -(b_{21}u_x + b_{22}u_y). \end{aligned} \tag{2}$$

The coefficients a_i, b_{ij} are known functions of x, y, and t. For future reference we also introduce

$$\mathbf{a} = (a_1, a_2), \quad \mathbf{F} = (F, G), \quad \mathbf{n} = (n_1, n_2), \quad B = \begin{bmatrix} b_{11} & b_{12} \\ b_{21} & b_{22} \end{bmatrix}, \tag{3}$$

where $\boldsymbol{n}$ is the outward pointing unit normal on $\delta\Omega$. We also demand that

$$x^T(B + B^T)x \geq 0. \tag{4}$$

Equation (1) can be thought of as a model for the Euler, Navier–Stokes, or Maxwell's equations.

We consider the following concepts of well-posedness and stability (see [25]).

DEFINITION 1. The problem (1) is strongly well posed if the solution u is unique, exists, and satisfies

$$\|u\|_\Omega^2 + \int_0^t \|u\|_{\delta\Omega}^2\, dt \leq K_c e^{\eta_c t} \left\{ \|f\|_\Omega^2 + \int_0^t \left(\|h\|_\Omega^2 + \|g\|_{\delta\Omega}^2 \right) dt \right\}, \tag{5}$$

where K_c and η_c may not depend on h, f, g, and $\|\cdot\|_\Omega$ and $\|\cdot\|_{\delta\Omega}$ are suitable continuous norms.

DEFINITION 2. The numerical approximation of (1) is strongly stable if for a sufficiently fine mesh the approximative solution U satisfies

$$\|U\|_\Omega^2 + \int_0^t \|U\|_{\delta\Omega}^2\, dt \leq K_d e^{\eta_d t} \left\{ \|f\|_\Omega^2 + \int_0^t \left(\|h\|_\Omega^2 + \|g\|_{\delta\Omega}^2 \right) dt \right\}, \tag{6}$$

where K_d and η_d may not depend on h, f, g, and $\|\cdot\|_\Omega$ and $\|\cdot\|_{\delta\Omega}$ are suitable discrete norms.

DEFINITION 3. The numerical approximation of (1) is strictly stable if the analytical and discrete growth rates (see (5) and (6)) satisfy

$$\eta_d \leq \eta_c + \mathcal{O}(\Delta x), \tag{7}$$

where Δx is the mesh size.

The ambition in this paper is to develop a strictly stable high-order procedure for (1) in curvilinear coordinates. In so doing, the difficulties presented by the combination of multiple dimensions and varying coefficients will be analyzed. Our strategy is to mimic the continuous procedure as closely as possible. The main analytical tool, i.e., the energy method, leads to

$$\|\Phi\|_t^2 = \mathrm{BT} + \mathrm{GR1} + \mathrm{GR2} + \mathrm{DI} + \mathrm{IT}, \tag{8}$$

where Φ stands for the continuous or discrete solution. BT, GR1, GR2, and DI denote boundary terms, growth terms due to varying wave speeds, growth terms due to forcing, and dissipation, respectively. IT denotes interface terms and exists only in the discrete case. The terms in (8) will be studied closely below.

3. THE CONTINUOUS PROBLEM

Consider the problem (1) on a curvilinear domain. By introducing the transformation $t = \tau, x = x(\xi, \eta), y = y(\xi, \eta)$ and its inverse $\tau = t, \xi = \xi(x, y), \eta = \eta(x, y)$, the new problem becomes

$$\begin{aligned} Ju_r + (\hat{F})_\xi + (\hat{G})_\eta &= \hat{h}, \quad [\xi, \eta] \in \hat{\Omega}, \quad \tau \geq 0, \\ u &= f, \quad [\xi, \eta] \in \hat{\Omega}, \quad \tau = 0, \\ \hat{L}u &= \hat{g}, \quad [\xi, \eta] \in \delta\hat{\Omega}, \quad \tau \geq 0, \end{aligned} \tag{9}$$

where $\hat{h} = Jh,\ f, \hat{g}$ are the data of the problem and $\hat{\Omega} = [\xi, \eta] \in [-1, 1] \times [0, 1]$. The new transformed fluxes are

$$\begin{aligned} \hat{F} &= J(\mathbf{F} \cdot \nabla\xi) = \hat{F}^I + \hat{F}^V, \quad \hat{F}^I = \hat{a}_1 u, \quad \hat{F}^V = -[\hat{b}_{11} u_\xi + \hat{b}_{12} u_\eta], \\ \hat{G} &= J(\mathbf{F} \cdot \nabla\eta) = \hat{G}^I + \hat{G}^V, \quad \hat{G}^I = \hat{a}_2 u, \quad \hat{G}^V = -[\hat{b}_{21} u_\xi + \hat{b}_{22} u_\eta], \end{aligned} \tag{10}$$

where

$$\begin{aligned} \hat{a}_1 &= J\mathbf{a} \cdot \nabla\xi, \quad \hat{b}_{11} = J\nabla\xi^T \cdot B\nabla\xi, \quad \hat{b}_{12} = J\nabla\xi^T \cdot B\nabla\eta, \\ \hat{a}_2 &= J\mathbf{a} \cdot \nabla\eta, \quad \hat{b}_{21} = J\nabla\eta^T \cdot B\nabla\xi, \quad \hat{b}_{22} = J\nabla\eta^T \cdot B\nabla\eta \end{aligned} \tag{11}$$

and B is given in (3). For later reference we include the metric relations

$$\begin{aligned} J\xi_x &= y_\eta, \quad J\xi_y = -x_\eta, \quad J = x_\xi y_\eta - x_\eta y_\xi, \\ J\eta_x &= -y_\xi, \quad J\eta_y = x_\xi, \quad J = (\xi_x \eta_y - \xi_y \eta_x)^{-1}. \end{aligned} \tag{12}$$

3.1. The Energy Method

Let

$$(u,v)_J = \int_0^1 \int_{-1}^1 (uv) J \, d\xi \, d\eta, \quad \|u\|_J^2 = (u,u)_J, \tag{13}$$

$$(u,v) = \int_0^1 \int_{-1}^1 (uv) \, d\xi \, d\eta, \quad \|u\|^2 = (u,u), \tag{14}$$

$$(u,v)_{E,W} = \int_0^1 (uv)_{E,W} \, d\eta, \quad \|u\|_{E,W}^2 = (u,u)_{E,W}, \tag{15}$$

$$(u,v)_{N,S} = \int_{-1}^1 (uv)_{N,S} \, d\xi, \quad \|u\|_{N,S}^2 = (u,u)_{N,S} \tag{16}$$

denote the weighted L_2 scalar product and norm, the L_2 scalar product and norm, the boundary scalar products, and boundary norms, respectively. The subscripts E, W, N, and S refer to the EAST, WEST, NORTH, and SOUTH boundaries, as in Fig. 1.

The energy-method applied to (9) leads to

$$\begin{aligned}
\left(\|u\|_J^2\right)_\tau = &-\underbrace{[(u, \hat{F}^I + 2\hat{F}^V)_E - (u, \hat{F}^I + 2\hat{F}^V)_W]}_{\text{EAST-WEST}} \\
&-\underbrace{[(u, \hat{G}^I + 2\hat{G}^V)_N - (u, \hat{G}^I + 2\hat{G}^V)_S]}_{\text{NORTH-SOUTH}} \\
&-\underbrace{\left[\left(u, \hat{F}^I_\xi\right) - (u_\xi, \hat{F}^I) + \left(u, \hat{G}^I_\eta\right) - (u_\eta, \hat{G}^I)\right]}_{\text{GR1}} + \underbrace{[(u, \hat{h}) + (\hat{h}, u)]}_{\text{GR2}} \\
&+\underbrace{[(u_\xi, \hat{F}^V) + (\hat{F}^V, u_\xi) + (u_\eta, \hat{G}^V) + (\hat{G}^V, u_\eta)].}_{\text{DI}}
\end{aligned} \tag{17}$$

GR1 and GR2 in (17) can lead to a growth or decay in $\|u\|_J^2$ but will not affect well-posedness; they can be estimated as

$$\text{GR1} \le \eta_{1c}\|u\|^2, \quad \text{GR2} \le \eta_{2c}\|u\|^2 + \frac{1}{\eta_{2c}}\|\hat{h}\|^2. \tag{18}$$

The metric relations (12) show that GR1 vanishes for constant-coefficient problems. To bound $\|u\|_J^2$ in time, the first two terms must be bounded using the correct boundary

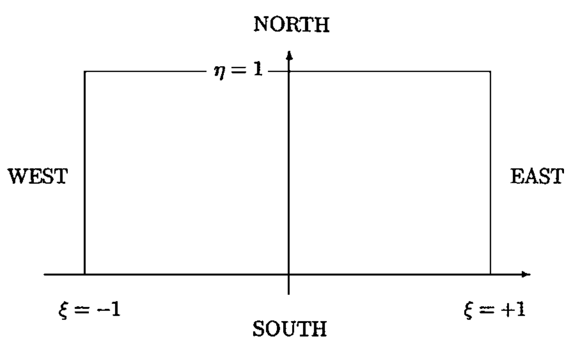

FIG. 1. The computational domain.

conditions and the dissipation DI must have the right sign. The introduction of $v = (u_\xi, u_\eta)^T$, $T = (\nabla_\xi, \nabla_\eta)$ leads to (see Eqs. (17), (10), and (11))

$$\mathrm{DI} = -J(Tv)^T(B + B^T)(Tv) \leq 0 \tag{19}$$

since (4) holds.

3.2. Boundary Conditions

Consider the first two terms in (17) and recall the definitions (3). The outward pointing unit normal on $\delta\hat{\Omega}$ is

$$\mathbf{n}(\xi = \pm 1, \eta) = \frac{\pm\nabla\xi}{|\nabla\xi|}, \quad \mathbf{n}(\xi, \eta = 0, 1) = \frac{\mp\nabla\eta}{|\nabla\eta|}, \tag{20}$$

where $|\nabla\xi| = \sqrt{\xi_x^2 + \xi_y^2}$ and $|\nabla\eta| = \sqrt{\eta_x^2 + \eta_y^2}$. With piecewise continuous normals, the integration by parts procedure leading to (17) is well defined.

In [27] it is shown that the boundary conditions leading to an energy estimate become

$$\begin{aligned}
-\hat{a}_1(-1, \eta, t) &= -J\mathbf{a} \cdot \nabla\xi < 0, \quad J\mathbf{F} \cdot \nabla\xi = \hat{F} = \hat{F}_W(\eta, t), \\
-\hat{a}_1(-1, \eta, t) &= -J\mathbf{a} \cdot \nabla\xi \geq 0, \quad J\mathbf{F}^V \cdot \nabla\xi = \hat{F}^V = \hat{F}_W^V(\eta, t), \\
+\hat{a}_1(+1, \eta, t) &= J\mathbf{a} \cdot \nabla\xi \geq 0, \quad J\mathbf{F}^V \cdot \nabla\xi = \hat{F}^V = \hat{F}_E^V(\eta, t), \\
+\hat{a}_1(+1, \eta, t) &= J\mathbf{a} \cdot \nabla\xi < 0, \quad J\mathbf{F} \cdot \nabla\xi = \hat{F} = \hat{F}_E(\eta, t)
\end{aligned} \tag{21}$$

at $\xi = \pm 1$, while

$$\begin{aligned}
-\hat{a}_2(\xi, 0, t) &= -J\mathbf{a} \cdot \nabla\eta < 0, \quad J\mathbf{F} \cdot \nabla\eta = \hat{G} = \hat{G}_S(\xi, t), \\
-\hat{a}_2(\xi, 0, t) &= -J\mathbf{a} \cdot \nabla\eta \geq 0, \quad J\mathbf{F}^V \cdot \nabla\eta = \hat{G}^V = \hat{G}_S^V(\xi, t), \\
+\hat{a}_2(\xi, 1, t) &= J\mathbf{a} \cdot \nabla\eta \geq 0, \quad J\mathbf{F}^V \cdot \nabla\eta = \hat{G}^V = \hat{G}_N^V(\xi, t), \\
+\hat{a}_2(\xi, 1, t) &= J\mathbf{a} \cdot \nabla\eta < 0, \quad J\mathbf{F} \cdot \nabla\eta = \hat{G} = \hat{G}_N(\xi, t)
\end{aligned} \tag{22}$$

should be used at $\eta = 0, 1$. A compact formulation of (21) and (22) (see also [24]) is

$$\mathbf{a} \cdot \mathbf{n} \leq 0 \Rightarrow \mathbf{F} \cdot \mathbf{n} = \mathbf{F}_{\delta\Omega} \cdot \mathbf{n}, \quad \mathbf{a} \cdot \mathbf{n} > 0 \Rightarrow \mathbf{F}^V \cdot \mathbf{n} = \mathbf{F}_{\delta\Omega}^V \cdot \mathbf{n}. \tag{23}$$

In [27] it is shown that the boundary conditions (21), (22), (23) leads to the estimate

$$\left(\|u\|_J^2\right)_\tau \leq \sum_{I=E,W,N,S} \frac{1}{\eta_I} \|\tilde{F}_I\|_I^2 + \mathrm{GR1} + \mathrm{GR2} + \mathrm{DI}, \tag{24}$$

where

$$\begin{aligned}
\tilde{F}_E &= \sigma_1 \hat{F}_E + (1 - \sigma_1)\hat{F}_E^V, \quad \sigma_1 = (1 - |\hat{a}_1|/\hat{a}_1)/2, \\
\tilde{F}_W &= \sigma_3 \hat{F}_W + (1 - \sigma_3)\hat{F}_W^V, \quad \sigma_3 = -(1 + |\hat{a}_1|/\hat{a}_1)/2, \\
\tilde{G}_N &= \sigma_5 \hat{G}_N + (1 - \sigma_5)\hat{G}_N^V, \quad \sigma_5 = (1 - |\hat{a}_2|/\hat{a}_2)/2, \\
\tilde{G}_S &= \sigma_7 \hat{G}_S + (1 - \sigma_7)\hat{G}_S^V, \quad \sigma_7 = -(1 + |\hat{a}_2|/\hat{a}_2)/2
\end{aligned} \tag{25}$$

and

$$\eta_{E,W} = \frac{\int_0^1 |\hat{a}_1| u^2 \, d\eta}{\int_0^1 u^2 \, d\eta}\Bigg|_{\xi=1,-1}, \quad \eta_{N,S} = \frac{\int_{-1}^1 |\hat{a}_2| u^2 \, d\xi}{\int_{-1}^1 u^2 \, d\xi}\Bigg|_{\eta=1,0.}$$

The parameters η_E, η_W, η_N, η_S are strictly positive if $\hat{a}_1, \hat{a}_2$ are zero for a finite number of points. For vanishing wave speeds in (25) we define $\sigma_i(\hat{a}_1 = 0) = 0$, $i = 1, 3$ and $\sigma_i(\hat{a}_2 = 0) = 0$, $i = 5, 7$.

Time-integration of the estimate (24) leads to an energy estimate of the form (5) if (19) holds. Provided that a solution exists we can conclude that the following theorem holds.

THEOREM 1. *Problem* (9), (21), (22) *is strongly well posed.*

3.3. Treatment of Corners

At the corners of the computational domain, the normals are discontinuous and extra care is required. As an example, the value of **n** close to the NORTH-EAST corner (see Fig. 1) is given by

$$\mathbf{n}_N(1,1) = \lim_{\delta \to 0^+} \mathbf{n}(1-\delta, 1), \quad \mathbf{n}_E(1,1) = \lim_{\delta \to 0^+} \mathbf{n}(1, \eta = 1-\delta). \tag{26}$$

The normals close to the other corners are defined in a similar way. The metric coefficients at the corners are well defined. Once the corner values of the metric coefficients, the normals, the wave vector, and the fluxes (see (20), (10), (11)) are well defined, condition (23) can be applied.

Another aspect of corner treatment is the boundary data compatibility. Consider the generally formulated problem $P(u_\tau, u_\xi, u_\eta, u_{\xi\xi}, u_{\xi\eta}, u_{\eta\eta}) = 0$, where P is a linear differential operator with boundary conditions $\tilde{F}(u, u_\xi, u_\eta) = f(1, \eta, \tau)$ and $\tilde{G}(u, u_\xi, u_\eta) = g(\xi, 1, \tau)$ close to the NORTH-EAST corner. We can differentiate $\tilde{F}$, f with respect to η, τ and $\tilde{G}$, g with respect to ξ, τ. By doing that and using $P = 0$ to reduce the number of unknowns, we obtain a matrix equation of the form $AU = H$, where $U = [u, u_\tau, u_\xi, u_\eta, u_{\xi\eta}, \ldots]^T$ and $H = [f, g, f_\tau, g_\tau, f_\eta, g_\xi, \ldots]^T$.

The rows of A are given by the coefficients in P, $\tilde{F}$, and $\tilde{G}$. The number of compatibility conditions are given by the number of linearly dependent rows in A. With two (or more) rows identical in A, the corresponding components in H must also be identical; that identity is called a compatibility condition.

As an example, consider Laplaces equation $u_{\xi\xi} + u_{\eta\eta} = 0$ close to the NORTH-EAST corner augmented with $\tilde{F} = \alpha_1 u + \beta_1 u_\xi$, $\tilde{G} = \alpha_2 u + \beta_2 u_\eta$. The relations $\tilde{F} = f$, $\tilde{G} = g$, and $\tilde{F}_\eta = f_n$, $\tilde{G}_\xi = g_\xi$ lead to

$$\begin{bmatrix} \alpha_1 & \beta_1 & 0 & 0 \\ \alpha_2 & 0 & \beta_2 & 0 \\ 0 & 0 & \alpha_1 & \beta_1 \\ 0 & \alpha_2 & 0 & \beta_2 \end{bmatrix} \begin{bmatrix} u \\ u_\xi \\ u_\eta \\ u_{\xi\eta} \end{bmatrix} = \begin{bmatrix} f \\ g \\ f_\eta \\ g_\xi \end{bmatrix} \Leftrightarrow \begin{bmatrix} \alpha_1\alpha 2 & 0 & 0 & -\beta_1\beta_2 \\ \alpha_1\alpha 2 & 0 & 0 & -\beta_1\beta_2 \\ 0 & 0 & \alpha_1 & \beta_1 \\ 0 & \alpha_2 & 0 & \beta_2 \end{bmatrix} \begin{bmatrix} u \\ u_\xi \\ u_\eta \\ u_{\xi\eta} \end{bmatrix}$$

$$= \begin{bmatrix} \alpha_2 f - \beta_1 g_\xi \\ \alpha_1 g - \beta_2 f_\eta \\ f_\eta \\ g_\xi \end{bmatrix}$$

Obviously $\alpha_2 f - \beta_1 g_\xi = \alpha_1 g - \beta_2 f_\eta$ is required (the compatibility condition). Higher order compatibility conditions are obtained by considering higher derivatives of P, $\tilde{F}$, and $\tilde{G}$.

Remark. As was shown above, it is an algebraically complex procedure to explicitly formulate the compatibility relations, even for simple model problems. However, compatibility is guaranteed if the same continuous solution is used to provide data for both f and g. In that case we have $f(1,\eta,\tau) = h(1,\eta,\tau)$, $g(\xi,1,\tau) = h(\xi,1,\tau)$. At far-field boundaries that situation often occurs since $h = h_\infty = const.$ is a common choice.

3.4. Interface Conditions

Boundary and interface conditions of the flux type (see (21) and (22)) require extra careful treatment; see [28] for an example.

3.4.1. *Interface Conditions in the Curvilinear Case*

To apply the Simultaneous Approximation Term (SAT) technique [16] on the fluxes at an interface between two blocks with different coordinate transformations and matching gridlines (see [17], [18] for the 1D treatment) requires that we identify the continuous part. Matching gridlines at $\xi = \xi_0 = \text{const}$ implies

$$(x_\xi)_1 \neq (x_\xi)_2, \quad (y_\xi)_1 \neq (y_\xi)_2, \quad (x_\eta)_1 = (x_\eta)_2, \quad (y_\eta)_1 = (y_\eta)_2 \tag{27}$$

while we have

$$(x_\xi)_1 = (x_\xi)_2, \quad (y_\xi)_1 = (y_\xi)_2, \quad (x_\eta)_1 \neq (x_\eta)_2, \quad (y_\eta)_1 \neq (y_\eta)_2 \tag{28}$$

at $\eta = \eta_0 = \text{const}$. The subscripts 1, 2 refer to the two coordinate transformations.

Equations (10), (12) and (27), (28) immediately lead to the conclusion that

$$\hat{F}_1(\xi_0,\eta,\tau) = \hat{F}_2(\xi_0,\eta,\tau), \quad \hat{G}_1(\xi_0,\eta,\tau) \neq \hat{G}_2(\xi_0,\eta,\tau), \tag{29}$$

$$\hat{F}_1(\xi,\eta_0,\tau) \neq \hat{F}_2(\xi,\eta_0,\tau), \quad \hat{G}_1(\xi,\eta_0,\tau) = \hat{G}_2(\xi,\eta_0,\tau); \tag{30}$$

i.e., $\hat{F}$ is continuous across $\xi = \text{const}$ while $\hat{G}$ is continuous across $\eta = \text{const}$.

3.4.2. *Interface Conditions and Vanishing Wave Speeds*

Another problem with flux-interface conditions appears when the wave speed a goes to zero. Consider the two constant-coefficient problems

$$u_t + F(u)_x = 0, \quad -L \le x \le 0 \quad \text{and} \quad v_t + F(v)_x = 0, \quad 0 \le x \le L,$$

where $F(w) = aw + F^V(w)$ and $F^V(w) = -\epsilon w_x$. Both problems have homogeneous outer boundary conditions at $|x| = L$ and zero initial data, and they are connected through interface conditions at $x = 0$. We will compare the effects of flux-interface conditions $(F(u) = F(v),\ F^V(u) = F^V(v))$ and variable-interface conditions $(u = v,\ u_x = v_x)$ on the solutions.

By transforming the problem for v on $[0, +L]$ onto $[-L, 0]$ via the transformation $x \to -\xi$, and then replacing ξ with x, we obtain

$$\psi_t + \Lambda\psi_x = \epsilon\psi_{xx}, \tag{31}$$

where $\psi = (u, v)^T$, $\Lambda = \mathrm{diag}(a, -a)$, and $B_{-L}\psi = 0$ denotes the outer boundary conditions at $x = -L$. $B_0\psi = 0$ represents the transformed interface conditions

$$au - \epsilon u_x = av + \epsilon v_x, \quad -\epsilon u_x = +\epsilon v_x \quad \text{or} \quad u = v, \quad u_x = -v_x. \tag{32}$$

We will treat (31) as a half-plane problem, which means that we let $L \to \infty$ and replace the influence of B_{-L} by only admitting bounded solutions as $x \to -\infty$.

The Laplace-transform technique applied to (31) leads to

$$\tilde{u}(x, s) = \sigma_1(s)\exp(\kappa_1(s)x), \quad \tilde{v}(x, s) = \sigma_2(s)\exp(\kappa_2(s)x),$$

where s is the dual variable with respect to time and

$$\kappa_1 = +\frac{a}{2\epsilon} + \sqrt{\left(\frac{a}{2\epsilon}\right)^2 + \frac{s}{\epsilon}}, \quad \kappa_2 = -\frac{a}{2\epsilon} + \sqrt{\left(\frac{a}{2\epsilon}\right)^2 + \frac{s}{\epsilon}}.$$

Note that both $\tilde{u}$ and $\tilde{v}$ decay away from the boundary $x = 0$.

The interface conditions (32) lead to the equation $E(s)\vec{\sigma} = 0$ where $\vec{\sigma} = (\sigma_1, \sigma_2)^T$. A well-posed bounded solution is obtained only if $\det(E(s)) \neq 0$ for $\Re(s) > 0$. The flux-interface and variable-interface conditions in (32) lead to

$$\det(E_f(s)) = -2\epsilon a\sqrt{\left(\frac{a}{2\epsilon}\right)^2 + \frac{s}{\epsilon}}, \quad \det(E_v(s)) = 2\sqrt{\left(\frac{a}{2\epsilon}\right)^2 + \frac{s}{\epsilon}} \tag{33}$$

respectively. Obviously the flux-interface conditions can lead to unbounded growth for vanishing wave speeds, because $\det(E_f)_{a\to 0} = 0$ independent of s. The variable-interface conditions, on the other hand, lead to a well-posed problem since $\det(E_v)_{a\to 0} = 2\sqrt{(s/\epsilon)}$.

A similar analyzis of the flux-boundary condition $au - \epsilon u_x = 0$ for the single domain yields $\det(E(s)) = a/2 + \sqrt{(a/2)^2 + s\epsilon}$. Consequently, the problem with unbounded growth for vanishing wave speed does not exist in the boundary condition case because $\det(E)_{a\to 0} = \sqrt{(s\epsilon)}$.

Remark. As a consequence of the investigation above, we will use flux conditions at outer boundaries and variable conditions or a combination of variable and flux conditions (see the *Remark* at the end of Section 4.3.2) at interfaces.

4. THE DISCRETE PROBLEM

Let the $N \times N$ matrix P_ξ and the $M \times M$ matrix P_η be 1D symmetric positive definite matrices with blocks in the upper left and lower right corner, see [27]. A product av can be

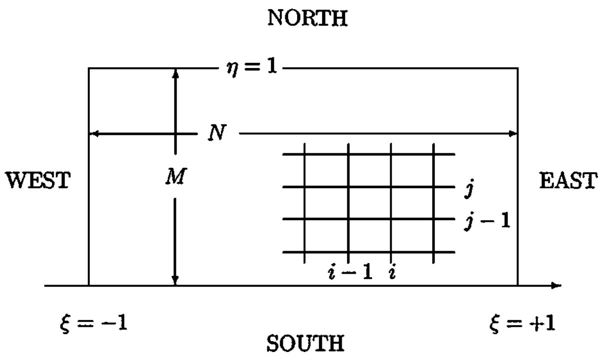

FIG. 2. The single domain case in transformed space.

arranged discretely (where $av \approx AV$) as (see Fig. 2)

$$AV = \begin{bmatrix} \tilde{A}_1 & & & & \\ & \tilde{A}_2 & & \mathbf{0} & \\ & & \ddots & & \\ & \mathbf{0} & & \tilde{A}_{N-1} & \\ & & & & \tilde{A}_N \end{bmatrix} \begin{bmatrix} \tilde{V}_1 \\ \tilde{V}_2 \\ \vdots \\ \tilde{V}_{N-1} \\ \tilde{V}_N \end{bmatrix}, \quad \tilde{V}_i = \begin{bmatrix} V_{i1} \\ V_{i2} \\ \vdots \\ V_{iM-1} \\ V_{iM} \end{bmatrix}, \tag{34}$$

where $\tilde{A}_i = \mathrm{diag}(a_{ij})$. Also, the $N \times N$ matrices J_E, J_W, I_ξ and the $M \times M$ matrices J_N, J_S, I_η have the form

$$J_{E,N} = \begin{bmatrix} 0 & \cdots & 0 \\ \vdots & \ddots & \vdots \\ 0 & \cdots & 1 \end{bmatrix}, \quad J_{W,S} = \begin{bmatrix} 1 & \cdots & 0 \\ \vdots & \ddots & \vdots \\ 0 & \cdots & 0 \end{bmatrix}, \quad I_{\xi,\eta} = \begin{bmatrix} 1 & \cdots & 0 \\ \vdots & \ddots & \vdots \\ 0 & \cdots & 1 \end{bmatrix}. \tag{35}$$

The subscripts E, W, N, and S refers to the EAST, WEST, NORTH, and SOUTH boundaries (see Fig. 2).

4.1. The Norms

The norms and scalar- products corresponding to (13)–(16) are

$$(U, V)_J = U^T(P_\xi \otimes P_\eta) J V, \quad (U, U)_J = \|U\|_J^2, \tag{36}$$

$$(U, V) = U^T(P_\xi \otimes P_\eta) V, \quad (U, U) = \|U\|^2, \tag{37}$$

$$(U, V)_{E,W} = U^T(J_{E,W} \otimes P_\eta) V, \quad \|U\|_{E,W}^2 = (U, U)_{E,W}, \tag{38}$$

$$(U, V)_{N,S} = U^T(P_\xi \otimes J_{N,S}) V, \quad \|U\|_{N,S}^2 = (U, U)_{N,S}. \tag{39}$$

Obviously, the relations (37)–(39) define norms since P_ξ and P_η are positive definite matrices. What about $(P_\xi \otimes P_\eta) J$ in (36)?

The metric scalar J is defined in (12). In matrix formulation we have

$$J = \mathrm{diag}(\tilde{J}_i), i = 1, \ldots, N \quad \tilde{J}_i = \mathrm{diag}(J_{ij}), j = 1, \ldots, M. \tag{40}$$

In [27], the following lemma was shown to hold.

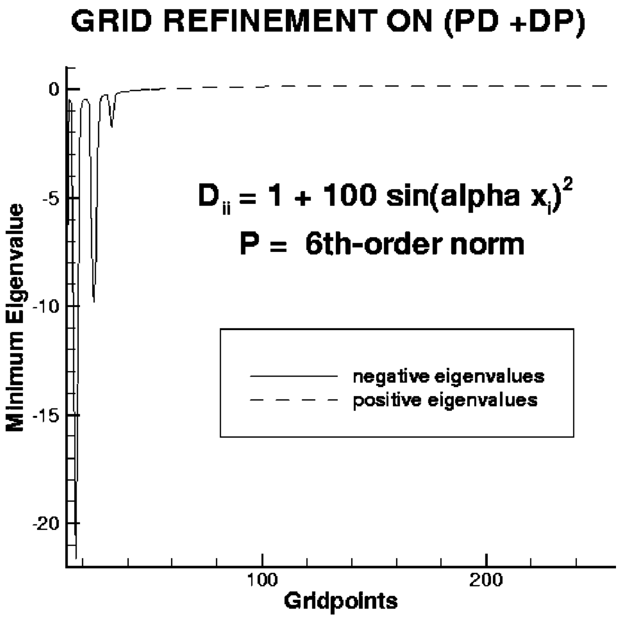

FIG. 3. Minimum eigenvalue of $PD + DP$ as a function of Δx.

LEMMA 1. *Let $M = P_\xi \otimes P_\eta$. If the first and last r components in $\tilde{J}_i$ are constants and the first $(\tilde{J}_1, \ldots, \tilde{J}_q)$ and last $(\tilde{J}_{N-(q-1)}, \ldots, \tilde{J}_N)$ q blocks in J are equal, then MJ is a norm.*

Remark. The conditions in Lemma 1 (i.e., that J must be constant in the first q, r points normal and adjacent to the boundary $\delta\Omega$) are theoretically ideal conditions. In practice one approaches the ideal condition with increasing resolution on a smooth mesh close to the boundary because

$$\begin{aligned} J(i, j) - J(0, j) &= J_\xi(0, \eta_j)(i\Delta\xi) + \mathcal{O}(\Delta\xi^2), \quad i = 1, \ldots, q, \\ J(i, j) - J(i, 0) &= J_\eta(\xi_i, 0)(j\Delta\eta) + \mathcal{O}(\Delta\eta^2), \quad j = 1, \ldots, r, \end{aligned}$$

where it is assumed that $J(0, j)$, $J(i, 0)$ are the values of J at the boundaries. This process is illustrated in Fig. 3, where the minimum eigenvalue of $PD + DP$ as a function of increasing resolution is shown. The minimum eigenvalue goes from a negative value for large Δx to a positive one for small Δx.

Remark. With lower accuracy requirements (see [27]) we can use diagonal norms P_ξ, P_η, which guarantees that MJ is a norm for all J.

4.2. The Single-Domain Problem

The discrete formulation of (9), (21), (22) with the SAT technique [16] for incorporating flux boundary conditions is

$$JU_\tau + D_\xi F + D_\eta G = h + PT, \quad U(0) = f, \tag{41}$$

where the continuous derivatives F_ξ, G_η are approximated with

$$D_\xi F = \left(P_\xi^{-1} Q_\xi \otimes I_\eta\right) F, \quad D_\eta G = \left(I_\xi \otimes P_\eta^{-1} Q_\eta\right) G \tag{42}$$

and

$$\begin{aligned} PT = {} & \left(P_\xi^{-1} J_E \otimes I_\eta \Sigma_1\right)(F - F_E) + \left(P_\xi^{-1} J_E \otimes I_\eta \Sigma_2\right)\left(F^V - F_E^V\right) \\ & + \left(P_\xi^{-1} J_W \otimes I_\eta \Sigma_3\right)(F - F_W) + \left(P_\xi^{-1} J_W \otimes I_\eta \Sigma_4\right)\left(F^V - F_W^V\right) \\ & + \left(I_\xi \Sigma_5 \otimes P_\eta^{-1} J_N\right)(G - G_N) + \left(I_\xi \Sigma_6 \otimes P_\eta^{-1} J_N\right)\left(G^V - G_N^V\right) \\ & + \left(I_\xi \Sigma_7 \otimes P_\eta^{-1} J_S\right)(G - G_S) + \left(I_\xi \Sigma_8 \otimes P_\eta^{-1} J_S\right)\left(G^V - G_S^V\right). \end{aligned} \tag{43}$$

For notational simplicity, the "hat" notation for the fluxes and transformed coefficients introduced in (9)–(11) are omitted. The $N \times N$ matrix Q_ξ and the $M \times M$ matrix Q_η are defined below in (46). Fluxes with subscripts E, W, N, and S are boundary data. The matrices Σ_1–Σ_8 will be determined below.

Remark. In (43), compatible data in the sense that was discussed in Section 3.3 is used. Compatibility is a continuous issue; the discrete task is to impose the (compatible) data in a stable and accurate way.

4.2.1. *The Energy Method*

Multiplying (41) from the left with $U^T(P_\xi \otimes P_\eta)$, introducing the notation $M = P_\xi \otimes P_\eta$, and adding the transpose of the equation leads to

$$\left(\|U\|_J^2\right)_\tau = \mathrm{BT} + \mathrm{GR1} + \mathrm{GR2} + \mathrm{DI}, \tag{44}$$

where $\mathrm{BT} = \text{E-W} + \text{N-S} + (U, PT) + (PT, U)$ and

$$\begin{aligned} \text{E-W} &= -[U^T(B_\xi \otimes P_\eta)(F^I + 2F^V) + (F^I + 2F^V)^T(B_\xi \otimes P_\eta)U]/2, \\ \text{N-S} &= -[U^T(P_\xi \otimes B_\eta)(G^I + 2G^V) + (G^I + 2G^V)^T(P_\xi \otimes B_\eta)U]/2, \\ \mathrm{GR1} &= -[[(U, D_\xi F^I) + (D_\xi F^I, U)] - [(F^I, D_\xi U) + (D_\xi U, F^I)]]/2 \\ &\quad - [[(U, D_\eta G^I) + (D_\eta G^I, U)] - [(G^I, D_\eta U) + (D_\eta U, G^I)]]/2, \\ \mathrm{GR2} &= +[U^T M h + h^T M U], \\ \mathrm{DI} &= +[((D_\xi U, F^V) + (F^V, D_\xi U) + (D_\eta U), G^V) + (G^V, D_\eta U)]. \end{aligned} \tag{45}$$

In (44) we have assumed that the metric transformation is such that MJ is a norm. The notations and abbreviations

$$Q_\xi + Q_\xi^T = B_\xi = J_E - J_W, \quad Q_\eta + Q_\eta^T = B_\eta = J_N - J_S \tag{46}$$

have been used to expand (44).

Note the close similarity of the discrete energy estimate (44), (45) with the corresponding continuous one; see (17). Just as in the continuous case GR1 and GR2 will at most create an exponential time growth; they can be estimated as

$$\mathrm{GR1} \le \eta_{1d}\|U\|^2, \quad \mathrm{GR2} \le \eta_{2d}\|U\|^2 + \frac{1}{\eta_{2d}}\|h\|^2. \tag{47}$$

We make the following assumption.

ASSUMPTION 1. The bounds in the estimates (18) and (47) satisfy

$$\eta_{id} \leq \eta_{ic} + \mathcal{O}(\Delta\xi, \Delta\eta), \quad i = 1, 2. \tag{48}$$

To obtain an energy estimate we must determine under what conditions the dissipation (DI) is negative definite and which values we must assign to the matrices Σ_1–Σ_8 to obtain bounded contributions from the boundary.

4.2.2. *The Numerical Dissipation*

The DI (see (10) and (45)) is

$$\mathrm{DI} = -\begin{bmatrix} D_\xi U \\ D_\eta U \end{bmatrix} \begin{bmatrix} B_{11}M + MB_{11} & B_{21}M + MB_{12} \\ B_{12}M + MB_{21} & B_{22}M + MB_{22} \end{bmatrix} \begin{bmatrix} D_\xi U \\ D_\eta U \end{bmatrix}, \tag{49}$$

where $B_{kl}(i, j) = b_{kl}(\xi_i, \eta_j)$. In [27], the following lemma was shown to hold.

LEMMA 2. *If the boundary blocks H_ξ^L, H_ξ^R in P_ξ have the size $q \times q$, the boundary blocks H_η^L, H_η^R in P_η have the size $r \times r$, and the matrices B_{kl} in* (49) *are constant in the first q, r points normal and adjacent to the boundary $\delta\Omega$, then the dissipation DI defined in* (49) *is negative definite.*

Remark. The conditions in Lemma 2 (i.e., that the matrices B_{kl} in (49) are constant in the first q, r points normal and adjacent to the boundary $\delta\Omega$) are theoretically ideal conditions. In practice, one approaches the ideal condition with increasing resolution, smooth coefficients b_{ij} and a smooth mesh; see the two *Remarks* on J in Section 4.1.

4.2.3. *Boundary Conditions*

Let us estimate the terms at the EAST boundary. By collecting terms we get

$$\begin{aligned} \mathrm{BT}_E = &-\left\{U^T[P_\eta(I/2 - \Sigma_1)]F^I + (F^I)^T\left[\left(I/2 - \Sigma_1^T\right)P_\eta\right]U\right\} \\ &-\left\{U^T[P_\eta(I - \Sigma_1 - \Sigma_2)]F^V + (F^V)^T\left[\left(I - \Sigma_1^T - \Sigma_2^T\right)P_\eta\right]U\right\} \\ &-[U^T P_\eta \tilde{F}_E + (\tilde{F}_E)^T P_\eta U], \end{aligned}$$

where $\tilde{F}_E = \Sigma_1 F_E + \Sigma_2 F_E^V$.

Obviously, the terms involving the viscous fluxes must be removed. This yields $\Sigma_2 = I - \Sigma_1$. By observing that $F^I = \Lambda_E U$ where $\Lambda_E = \mathrm{diag}((\hat{a}_1)_{Nj})$ (see (11) for a definition of $\hat{a}_1$) we obtain

$$\mathrm{BT}_E = -U^T\left[P_\eta(I/2 - \Sigma_1)\Lambda_E + \Lambda_E\left(I/2 - \Sigma_1^T\right)P_\eta\right]U - [U^T P_\eta \tilde{F}_E + (\tilde{F}_E)^T P_\eta U].$$

Now we choose Σ_1 such that $(I/2 - \Sigma_1)\Lambda_E = |\Lambda_E|/2$. This choice and an entirely similar procedure at the other boundaries yields

$$\left(\|U\|_J^2\right)_\tau \leq \sum_{I=E,W,N,S} \frac{1}{\eta_I}\|\tilde{F}_I\|_I^2 + \mathrm{GR1} + \mathrm{GR2} + \mathrm{DI}, \tag{50}$$

where

$$\begin{aligned}
\tilde{F}_E &= \Sigma_1 F_E + (I_y - \Sigma_1) F_E^V, \quad \Sigma_1 = \left(I_y - |\Lambda_E|\Lambda_E^{-1}\right)/2, \\
\tilde{F}_W &= \Sigma_3 F_W + (I_y - \Sigma_3) F_W^V, \quad \Sigma_3 = -\left(I_y + |\Lambda_W|\Lambda_W^{-1}\right)/2, \\
\tilde{G}_N &= \Sigma_5 G_N + (I_x - \Sigma_5) G_N^V, \quad \Sigma_5 = \left(I_x - |\Lambda_N|\Lambda_N^{-1}\right)/2, \\
\tilde{G}_S &= \Sigma_7 G_S + (I_x - \Sigma_7) G_S^V, \quad \Sigma_7 = -\left(I_x + |\Lambda_S|\Lambda_S^{-1}\right)/2,
\end{aligned} \tag{51}$$

$$\Sigma_2 = I_y - \Sigma_1, \quad \Sigma_4 = -I_y - \Sigma_3, \quad \Sigma_6 = I_x - \Sigma_5, \quad \Sigma_8 = -I_x - \Sigma_7, \tag{52}$$

and

$$\eta_I = \frac{1}{2}\frac{(U, |\Lambda_I|U)_I + (|\Lambda_I|U, U)_I]}{(U, U)_I}, \quad I = E, W, N, S.$$

Note the close similarity between the numerical and continuous boundary procedure (see (25) and (51)). For vanishing wave speeds in (51) we follow the procedure in the continuous case (see the end of Section 3.2.) and define $\Sigma_i(\hat{a}_1 = 0) = 0, i = 1, 3$ and $\Sigma_i(\hat{a}_2 = 0) = 0, i = 5, 7$.

The similarity of the discrete energy estimate (50) with the corresponding continuous one (see (24)) implies strict stability. Time-integration of (50) leads to an estimate of the form (6) if Assumption 1 and Lemma 2 hold. We can conclude that the following theorem holds.

THEOREM 2. *The approximation* (41) *of the problem* (9), (21), (22) *is both strictly and strongly stable if Assumption* 1 *and Lemma* 2 *hold and* Σ_1–Σ_8 *are given by* (51) *and* (52).

4.3. The 1D Multiple-Domain Problem Revisited

Before we consider the 2D multiple-domain problem, let us once more look at the 1D multiple-domain problem considered in [17, 18].

4.3.1. *Derivation of the Q-Formulation for Interface Problems*

Consider the hyperbolic interface problem

$$u_t + u_x = 0, \quad -1 \leq x \leq 0 \quad \text{and} \quad v_t + v_x = 0, \quad 0 \leq x \leq 1 \tag{53}$$

augmented with suitable initial and boundary data and the interface condition $u = v$ at $x = 0$. The straightforward approximation of (53) is

$$\begin{aligned}
U_t + P_L^{-1} Q_L U &= P_L^{-1}(\sigma_L(U_N - V_0)e_N), \\
V_t + P_R^{-1} Q_R V &= P_R^{-1}(\sigma_R(V_0 - U_N)e_0),
\end{aligned} \tag{54}$$

where $U = (U_0, \ldots, U_N)^T$, $e_N = (0, \ldots, 0, 1)^T$, $V = (V_0, \ldots, V_M)^T$, and $e_0 = (1, 0 \ldots, 0)^T$.

The boundary terms from the left (L) and right (R) outer boundaries are ignored. The formulation (54) can also be written as

$$PW_t + (Q + \Sigma)W = 0, \tag{55}$$

where $W = (U, V)^T$, $P = \text{diag}(P_L, P_R)$, $Q = \text{diag}(Q_L, Q_R)$, and

$$\Sigma = \begin{bmatrix} 0 & & 0 \\ & \tilde{\Sigma} & \\ 0 & & 0 \end{bmatrix}, \quad \tilde{\Sigma} = \begin{bmatrix} -\sigma_L & +\sigma_L \\ +\sigma_R & -\sigma_R \end{bmatrix}. \tag{56}$$

We can now split up $Q + \Sigma$ into a symmetric and a skew-symmetric part as

$$Q + \Sigma = \underbrace{\frac{(Q+\Sigma) - (Q+\Sigma)^T}{2}}_{Q^{sk}} + \underbrace{\frac{(Q+\Sigma) + (Q+\Sigma)^T}{2}}_{D}.$$

The 2×2 blocks of Q^{sk} and D corresponding to the nonzero elements in Σ are

$$\tilde{Q}^{sk} = \frac{1}{2}\begin{bmatrix} 0 & (\sigma_L - \sigma_R) \\ -(\sigma_L - \sigma_R) & 0 \end{bmatrix}, \quad \tilde{D} = \frac{1}{2}\begin{bmatrix} 1 - 2\sigma_L & \sigma_L + \sigma_R \\ \sigma_L + \sigma_R & -1 - 2\sigma_R \end{bmatrix}.$$

Henceforth, the "tilde" sign will indicate the 4×4 block that couples the solutions in the left and right domains. Equation (55) now becomes

$$PW_t + (Q^{sk} + D)W = 0. \tag{57}$$

In [17] it was shown that (54) is conservative if $\sigma_R = \sigma_L - 1$. By introducing this condition in $\tilde{Q}^{sk}$ and $\tilde{D}$ we obtain the final form of the difference operator,

$$\tilde{Q}^{sk} = \frac{1}{2}\begin{bmatrix} 0 & 1 \\ -1 & 0 \end{bmatrix}, \quad \tilde{D} = \sigma \begin{bmatrix} 1 & -1 \\ -1 & 1 \end{bmatrix}, \tag{58}$$

where $\sigma = 1/2 - \sigma_L$.

The formulation (57), (58) hereafter referred to as the Q-formulation is a rearranged form of the original formulation (54). However, the Q-formulation simplifies and even extends the possibility to formulate suitable penalty terms for second-order derivatives.

4.3.2. *The Q-Formulation for Advection–Diffusion Interface Problems*

Consider

$$u_t + F(u)_x = 0, \quad -1 \leq x \leq 0 \quad \text{and} \quad v_t + F(v)_x = 0, \quad 0 \leq x \leq 1, \tag{59}$$

where $F(w) = a(x, t)w - \epsilon w_x$ augmented with suitable initial, boundary, and interface conditions. An approximation of (59) using the Q-formulation is

$$PW_t + (Q^{sk})(AW) - \epsilon(Q^{sk} + D_2)P^{-1}(Q^{sk} + D_3)W = D_1 W, \tag{60}$$

where $W = (U, V)^T$ and $P = \text{diag}(P_L, P_R)$. The matrix A has the values of $a(x_i, t)$ on the diagonal. The operator Q^{sk} is defined in Section 4.3.1., and

$$\tilde{D}_i = \sigma_i \begin{bmatrix} 1 & -1 \\ -1 & 1 \end{bmatrix}, \quad i = 1,\ 2,\ 3 \tag{61}$$

as in (58). The dissipation D_1 is formulated as acting on W, which is a more general formulation that includes penalty on the flux ($\sigma_1 = \sigma a(0, t)$) as well as penalty on the variables.

We can now prove

THEOREM 3. *The approximation* (60), (61) *of the problem* (59) *with the choices*

$$\sigma_1 \le 0, \quad \sigma_2 = 0, \quad \sigma_3 = 0 \tag{62}$$

is conservative and stable.

Proof. The energy method applied on (60) leads to

$$\|W\|_t^2 = \underbrace{(\mathcal{D}W, AW) - (\mathcal{D}(AW), W)}_{\text{GR1}} - \underbrace{2\epsilon(\mathcal{D}W, \mathcal{D}W)}_{\text{DI}} - \underbrace{W^T B(AW - 2\epsilon\mathcal{D}W)}_{\text{BT}} + \text{IT},$$

where $\mathcal{D}W = P^{-1}Q^{sk}W$ and the interface terms IT are defined as

$$\text{IT} = \begin{bmatrix} W \\ \mathcal{D}W \end{bmatrix}_0^T \begin{bmatrix} 2D_1 + 2\epsilon D_2 P^{-1} D_3 & \epsilon(D_2 - D_3) \\ \epsilon(D_2 - D_3) & 0 \end{bmatrix} \begin{bmatrix} W \\ \mathcal{D}W \end{bmatrix}_0. \tag{63}$$

The growth (GR1), the dissipation (DI), and the ordinary boundary terms (BT) match the terms in the corresponding continuous estimate perfectly. The choices (62) make the term IT maximally negative definite and lead to stability. The approximation (60) can now can be written

$$PW_t + Q^{sk}(AW - \epsilon P^{-1}Q^{sk}W) = D_1 W, \tag{64}$$

which leads to conservation. ■

Consider

$$PW_t + Q(AW - \epsilon P^{-1}QW) = (D_1 + (Q - Q^{sk})A)W + \epsilon(Q^{sk}P^{-1}Q^{sk} - QP^{-1}Q)W, \tag{65}$$

which is a formulation of (64) in the usual penalty form. The Q-formulation simplifies the construction of complex suitable penalty terms considerably.

Remark. The Q-formulation also removes the problem with vanishing wave speeds discussed in Section 3.4.2. To see this, let $\epsilon = 0$ in (65). Obviously, the amount of dissipation on the right-hand side of (65) is nonzero even if the wave speed $\boldsymbol{A} \to 0$. The Q-formulation can be considered to combine flux and variable interface conditions.

Remark. The linear continuous problem (1) considered in this paper does not of course produce any shocks. However, conservation is nevertheless a desirable property since we aim for a discrete approximation with the same behavior as the linear continuous problem, which indeed is conservative. In [18], it was shown that the conditions for conservation were a subset of the necessary conditions for stability. In this case, the situation is similar. The conservativion form (64) is obtained from (60) by letting $D_2 = D_3 = 0$, which obviously [see (63)] is necessary for stability since the (2, 2) element in the stability matrix is zero.

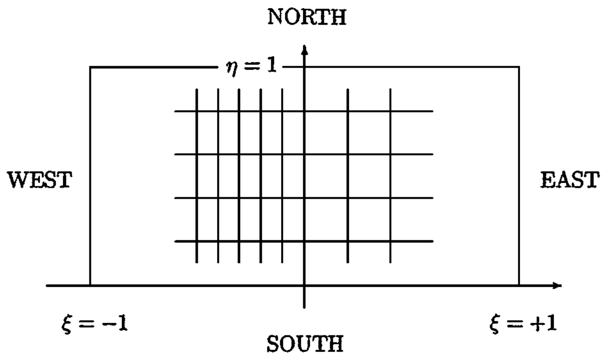

FIG. 4. The multiple domain mesh in transformed space.

4.4. The 2D Multiple-Domain Problem

In this section, an interface at $\xi = 0$ with matching gridlines (see Fig. 4) is considered. Matching gridlines implies that the number of points in the η direction (M) is the same on both sides of $\xi = 0$. We will also assume that $P_\eta^L = P_\eta^R = P_\eta$ and $Q_\eta^L = Q_\eta^R = Q_\eta$. The difference operators D_ξ^L, D_ξ^R can be different in the left and right domains and, in general, $\Delta\xi_L \neq \Delta\xi_R$ and $N_L \neq N_R$.

Remark. The treatment of two subdomains generalizes to an arbitrary number of adjoining 2D subdomains, in the ξ and/or η coordinates. The adjoining subdomains must have point matching gridlines, and the tangential differentiation operators at the interface must be identical. No corner point ambiguities exist at the discrete level, since the proofs of conservation and stability depend only on the interface treatment (including the corner point) and the two adjoining subdomains. In principle, an arbitrary number of subdomains can coincide at one point without causing ambiguities.

A multiple-domain Q-formulation of the problem (9), (21), (22) is

$$\bar{J} W_t + D_\xi^{sk} F + D_\eta G = \bar{M}^{-1}(D \otimes \Sigma P_\eta) W + h + PT, \quad W(0) = f, \tag{66}$$

where $W = (U, V)^T$. The solutions in the left (L) and right (R) domains are denoted, respectively, by U and V, and

$$D_\xi^{sk} = \bar{M}^{-1}\big(\bar{Q}_\xi^{sk} \otimes P_\eta\big), \quad D_\eta = \bar{M}^{-1}(\bar{P}_\xi \otimes Q_\eta). \tag{67}$$

In (66), PT denotes the boundary conditions in (41) at the NORTH, EAST, SOUTH, WEST boundaries in penalty form. The ξ derivatives in F, G are approximated with D_ξ^{sk}. The remaining definitions and notations used in (66) are $\bar{Q}_\xi^{sk} = \bar{Q}_\xi + \Delta$,

$$\bar{M} = \begin{bmatrix} M_L & 0 \\ 0 & M_R \end{bmatrix}, \quad \bar{J} = \begin{bmatrix} J_L & 0 \\ 0 & J_R \end{bmatrix}, \quad \bar{Q}_\xi = \begin{bmatrix} Q_\xi^L & 0 \\ 0 & Q_\xi^R \end{bmatrix}, \tag{68}$$

$$\Delta = \begin{bmatrix} 0 & 0 \\ & \tilde{\Delta} & \\ 0 & 0 \end{bmatrix}, \quad D = \begin{bmatrix} 0 & 0 \\ & \tilde{D} & \\ 0 & 0 \end{bmatrix}, \tag{69}$$

$$\bar{P}_\xi = \begin{bmatrix} P_\xi^L & 0 \\ 0 & P_\xi^R \end{bmatrix}, \quad \tilde{\Delta} = -\frac{1}{2}\begin{bmatrix} 1 & -1 \\ 1 & -1 \end{bmatrix}, \quad \tilde{D} = \begin{bmatrix} 1 & -1 \\ -1 & 1 \end{bmatrix}. \tag{70}$$

The matrix coefficient Σ will be determined by stability requirements.

The Q-formulation automatically leads to conservation:

THEOREM 4. *The approximation* (66) *of* (9), (21), (22) *is conservative.*

The proof of theorem 4 is given in [27]. We will now prove the following theorem.

THEOREM 5. *The approximation* (66) *of the problem* (9), (21), (22) *is both strictly and strongly stable if theorem* 2 *holds and* $\Sigma P_\eta + P_\eta \Sigma \leq 0$.

Proof. The energy method applied to (66) yields

$$\frac{d}{dt}\left(\|W\|_J^2\right) = \text{BT} + \text{GR1} + \text{GR2} + \text{DI} \ + \ \text{IT}, \tag{71}$$

where it is assumed that $\bar{M}\bar{J}$ is a norm; the requirements are given in Lemma 1. The boundary terms BT are exactly the same as in the single domain case (see (51)), while the D_ξ operator in GR1, GR2, and DI is replaced by D_ξ^{sk} defined in (67). Strict and strong stability of (66) follows if

$$\text{IT} = W^T D \otimes (\Sigma P_\eta + P_\eta \Sigma) W \leq 0. \tag{72}$$

Because $D \geq 0$, we need $\Sigma P_\eta + P_\eta \Sigma \leq 0$. ■

Remark. Because $P_\eta > 0$, $\Sigma \leq 0$ with the first and last r elements in Σ being constants would satisfy condition (72).

5. NUMERICAL EXPERIMENTS

The analysis in this paper deals with a scalar problem while interesting examples in most cases involve systems of equations. However, if a symmetrizer exists, most of the techniques in this paper (the energy method for boundary and interface conditions) can be used to analyze systems.

In the calculations below, we have used the fourth- and sixth-order schemes reported in [17] in space and a five-stage fourth-order Runge–Kutta (RK) scheme [30] in time. The penalty parameter σ in (58) is choosen to produce a suitable spectrum for the RK scheme. That often means $\sigma = 1/2$, which corresponds to maximum penalty on the downwind side. In terms of the original penalty parameters, [see (54)] it means $\sigma_L = 0$ and $\sigma_R = -1$.

5.1. Vanishing Wave Speed

For problems with a realistic geometry, one will frequently encounter zero wave speed somewhere in the field due to the variation of the metric coefficients, the variable coefficients, or (for nonlinear problems) the solution. This difficulty (see Section 3.4.2.), particularly severe in one dimension, is exemplified in the calculation of Burgers's equation shown in Fig. 5.

The instability that develops close to zero wave speed when using a penalty on the fluxes at the interfaces is evident. With interface conditions applied on the variable instead of

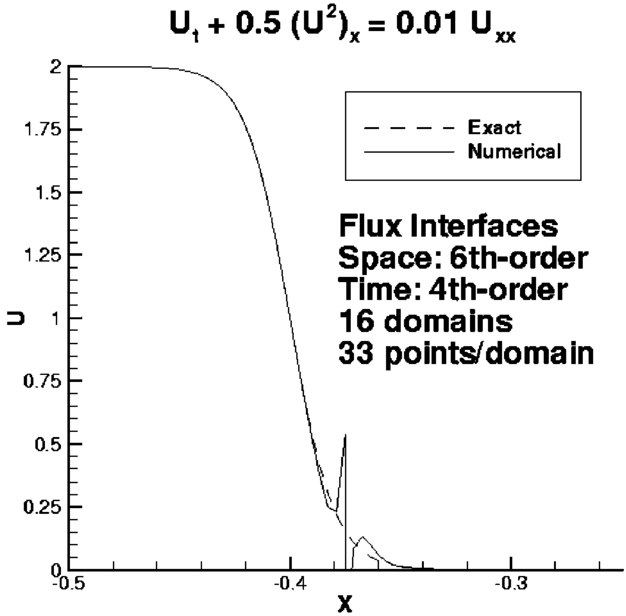

FIG. 5. Instability due to vanishing wave speed and flux interface conditions.

the fluxes or by using the Q-formulation, the instability disappears. Also, if one scales the problem such that U varies between 1 and 3 instead of 0 and 2 one can use flux interface conditions without any sign of instabilities. This anomalous behavior associated with a vanishing wave speed occurs with other numerical schemes and is typically suppressed by adding dissipation (e.g., the "entropy fix" used with Roe solvers).

5.2. Varying Wave Speed

The 1D Maxwell's equations with boundary conditions for a perfectly electric conductor are

$$\mu\frac{\partial H_y}{\partial t} = \frac{\partial E_z}{\partial x}, \quad \epsilon\frac{\partial E_z}{\partial t} = \frac{\partial H_y}{\partial x} - \sigma E_z, \quad E_z(0,t) = E_z(1,t) = 0. \tag{73}$$

By letting $\mu = \epsilon = 1, \sigma = 0$ and $u_1 = H_y - E_z, u_2 = H_y + E_z$ we obtain

$$u_t + F_x = 0, \quad [x, y] \in \Omega, \quad t \geq 0, \tag{74}$$

where $u = (u_1, u_2)^T$ and $F = (a(x)u_1, b(x)u_2)^T$. Note that we have introduced varying wave speeds and that the 1D problem is considered on the 2D domain $\Omega = [x, y] \in [0, 1] \times [0, 1]$.

The problem (74) is 1-periodic in y and has

$$u_1(0, y, t) = \alpha u_2(0, y, t), \quad u_2(1, y, t) = \beta u_1(1, y, t) \tag{75}$$

as boundary conditions in the x direction. For $a = 1, b = -1$ we have $\alpha = \beta = 1$, which corresponds to the boundary conditions in (73). By introducing a 2D curvilinear mesh we obtain

$$Ju_\tau + (\hat{F})_\xi + (\hat{G})_\eta = 0, \quad [\xi, \eta] \in \hat{\Omega}, \quad \tau \geq 0, \tag{76}$$

where $\hat{F} = J\xi_x F$, $\hat{G} = J\eta_x F$, and $\hat{\Omega} = [\xi, \eta] \in [0, 1] \times [0, 1]$. The problem (76) has the same boundary conditions as (74).

5.2.1. *The Energy Growth in 1D*

The energy growth for the 1D ($y = 0,\ \eta_x = 0$) version of (75), (76) with

$$a = 1 + \epsilon x, \quad b = -1 + \epsilon x, \quad \alpha = 1, \quad \beta = \sqrt{(1+\epsilon)/(1-\epsilon)} \tag{77}$$

leads to $\|u\|_t^2 = -\epsilon\|u\|^2$. The growth rate $-\epsilon/2$ corresponds to a single eigenvalue on the real axis in the continuous spectrum. Note that (75), (76) constitute an extremely sensitive test problem in which, one can specify the growth or decay of the solution exactly. Figure 6 shows the error in the sixth-order numerical approximation of this eigenvalue for different transformations ($x = x(\xi)$). Figure 7 shows the convergence (in an L_2 sense) of the seven eigenvalues with most accurately converged real parts. The convergence rate in both Figs. 6 and 7 is at least 6.

Even though the resolved eigenvalues (and eigenvectors) converge at the theoretical rate (see Figs. 6 and 7), there are unresolved eigenvalues and eigenvectors that can generate difficulties. In Fig. 8, the least resolved eigenvector corresponds to an eigenvalue with a negative real part (-4.6529×10^{-3}) significantly more to the right of the analytical value (-7.5000×10^{-3}) than could be expected by the order of the approximation. These unresolved eigenvalues and eigenvectors may generate extra energy growth. The difference

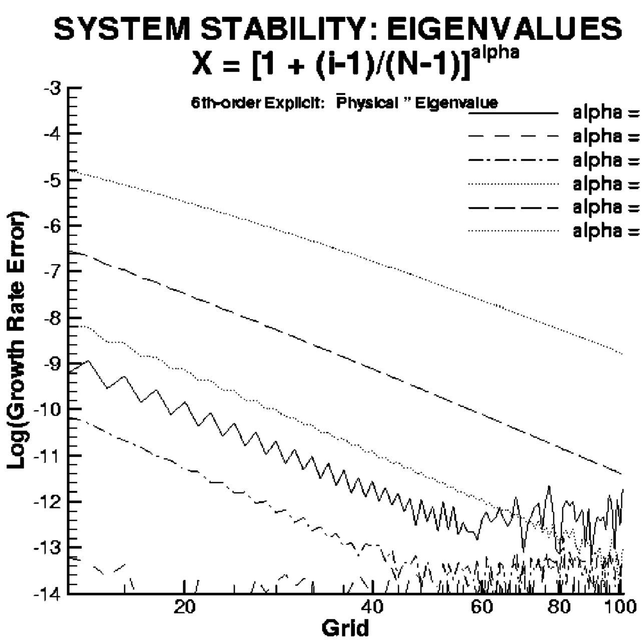

FIG. 6. The error in the growth rate for different transformations.

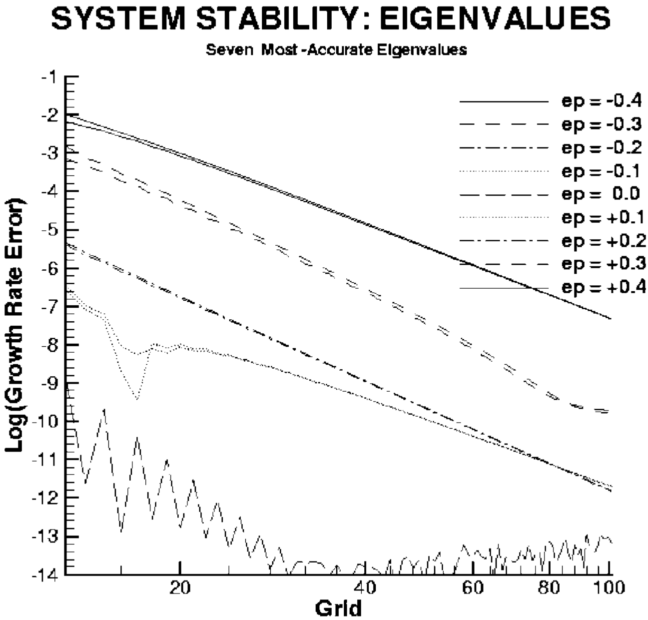

FIG. 7. The error in the growth rate for varying wave speeds.

between the growth rate in actual calculations and the analytical growth rate is shown in Fig. 9. As indicated in Fig. 8, the growth rate of the smooth sinusoidal initial functions converge to the analytical growth rate while there in no convergence for the nonsmooth sawtooth function. Ongoing work deals with adjusting the difference operators and moving the unresolved eigenvalues.

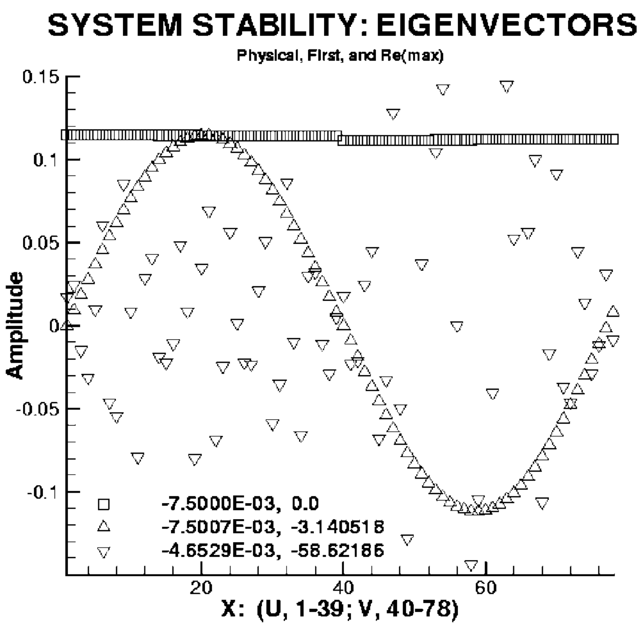

FIG. 8. Eigenvectors for the two most and the least resolved eigenvalues.

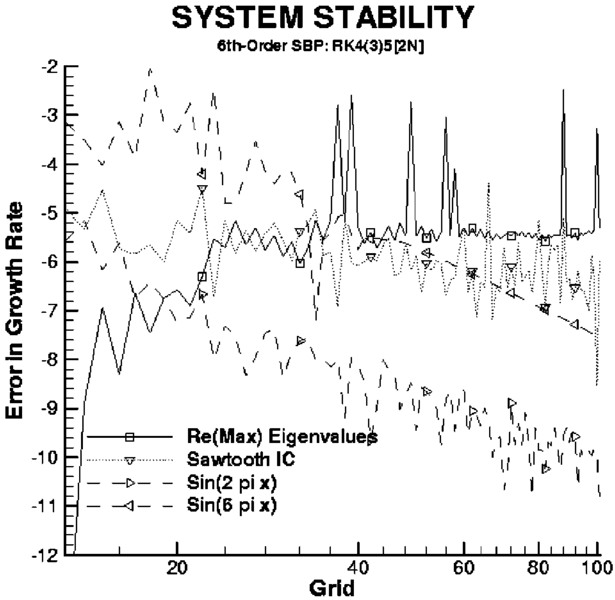

FIG. 9. Extra growth due to unresolved features and initial conditions.

5.2.2. *The Energy Growth in 2D*

The energy growth for the 2D continuous problems (75), (76) is identically zero with $\epsilon = 0$ in (77); i.e., the L_2 norm of the solution remains constant in time. In the semidiscrete case, the energy growth is given by (71) where GR2 = DI = 0, and the introduction of

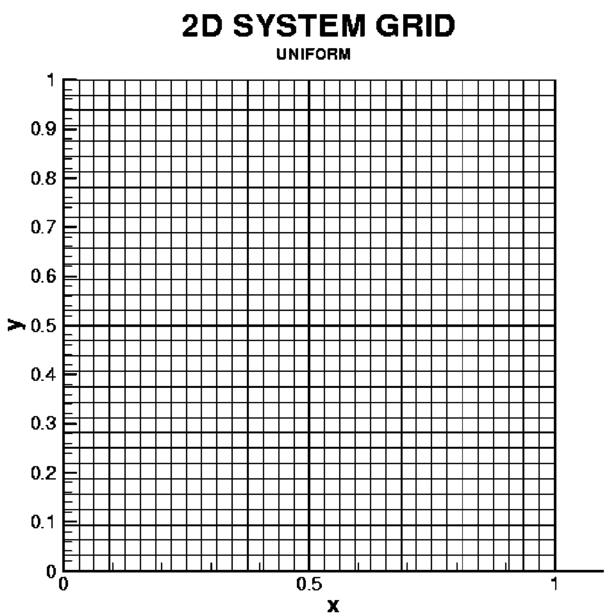

FIG. 10. A four-block mesh; linear mapping.

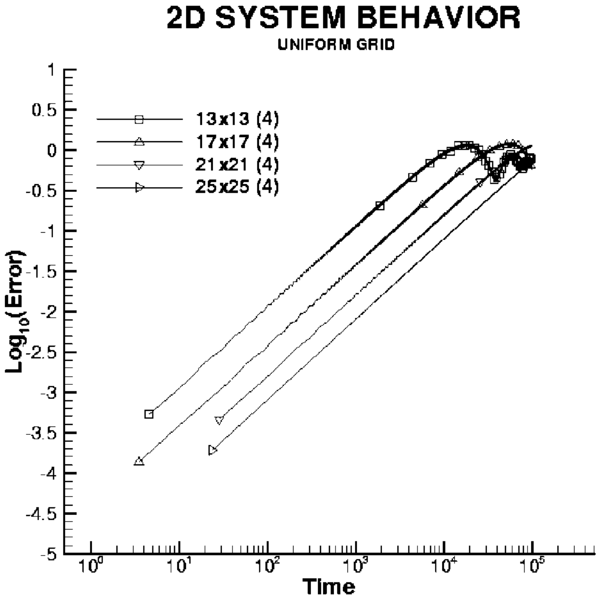

FIG. 11. Growth rates; linear mapping.

boundary conditions BT and interface conditions (IT) leads to damping. Possible error growth [see (45)] is provided by

$$GR1 = -[(U, D_\xi \hat{F}) - (D_\xi U, \hat{F})] - [(U, D_\eta \hat{G}) - (D_\eta U, \hat{G})] \tag{78}$$

only. For a uniform grid (see Fig. 10) we obtain GR1 = 0. The error growth (accumulation

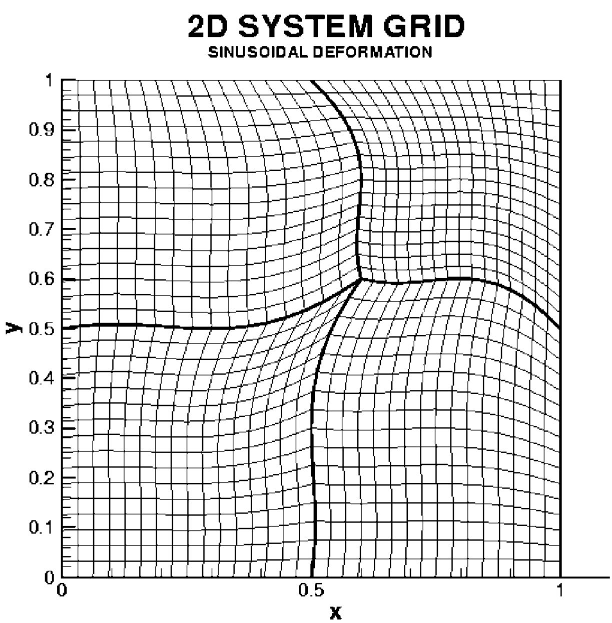

FIG. 12. A four-block mesh; nonlinear mapping.

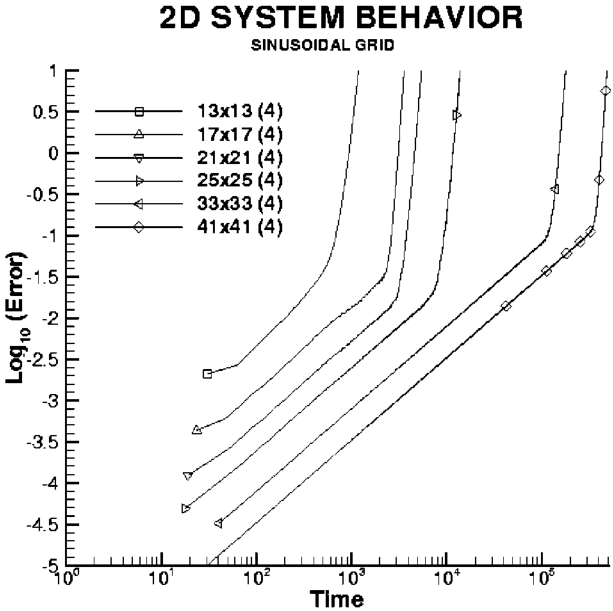

FIG. 13. Growth rates; nonlinear mapping.

of temporal error) is shown in Fig. 11. The calculations are fourth-order accurate in time. Note that there is an absolute bound on the error.

In a nonlinear mapping (see Fig. 12) the truncation errors in the metric calculation, and consequently also in the calculation of the fluxes, leads to GR1 $\neq 0$, which in turn can generate error growth which also includes an exponential character (see Fig. 13). Also in this case, we have fourth-order accuracy in time. Note the enormous time scale in Figs. 11 and 13.

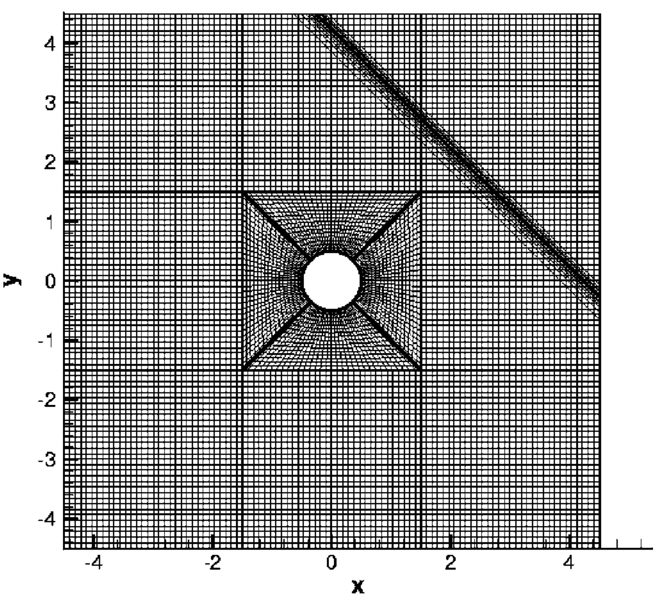

FIG. 14. Propagating viscous shock.

TABLE I
Twelve Subdomains, Sixth-order Explicit;
CFL = 0.3

Wave speed	49/65	65/97	97/129	129/193
−0.25	−4.610	−4.640	−4.722	−4.722
0.00	−5.115	−4.986	−4.538	−4.657
0.25	−5.155	−5.253	−5.179	−4.952
0.50	−5.331	−5.401	−5.467	−5.327
0.75	−5.523	−5.514	−5.590	−5.565
1.00	−5.635	−5.622	−5.659	−5.719
average	−5.228	−5.236	−5.193	−5.196

5.3. Navier–Stokes calculations

We consider here a 1D viscous shock propagating in accordance with a Mach number of 2.0 and a Reynolds number of 150 over a 2D domain. The exact solution of the Navier–Stokes equation for this case can be found in [31]. At the artificial boundaries, including the circular region in the middle, we impose flux boundary conditions by using the penalty formulation on the fluxes with exact data from the analytical solution. At the interfaces we impose interface conditions by using the penalty formulation on the variables.

In Fig. 14, the density and grid for the propagating shock is shown. The shock travels from the lower left corner to the upper right corner and has almost passed out of the computational domain that consists of 12 blocks. The sixth-order scheme and 24 gridpoints were used in each subdomain. The grid refinement study in Table I indicates between fifth- and sixth-order accuracy in an L_2 norm, consistent with the theory in [32, 33], since we have fifth-order accuracy at the boundaries and interfaces due to the repeated use of the first derivative operator and relatively coarse grids.

6. SUMMARY AND CONCLUSIONS

High-order finite difference methods applied to multidimensional linear problems in curvilinear coordinates have been analyzed. The investigation focused on the effect of variable coefficients.

The definition of normals and data compatibility at corners were discussed. Problems related to nondiagonal norms and a varying Jacobian were analyzed. A constant Jacobian in gridpoints close to the boundaries is required for nondiagonal norms. Dissipation with correct sign using nondiagonal norms requires a constant Jacobian and high resolution close to the boundaries.

Boundary and interface conditions in both flux and variable formulations have been investigated. Flux boundary conditions lead to energy estimates whereas flux interface conditions lead to difficulties for vanishing wave speeds.

A new and simplified so-called Q-formulation of the penalty method was derived at interfaces. The Q-formulation simplifies and extends the formulation and implementation of derivative conditions in both one and two dimensions at interfaces. The Q-formulation combines flux- and variable-interface conditions. The Q-formulation also removes the problem with vanishing wave speeds.

Varying wave speeds can cause additional error growth via the truncation errors even though the boundary and interface conditions are implemented in a stable and dissipative way. Numerical calculations confirmed the theoretical conclusions.

REFERENCES

1. R. L. Clark and K. D. Frampton, Aeroelastic structural acoustic coupling: Implications on the control of turbulent boundary-layer noise transmission, *J. Acoust. Soc. Am.* **102**, 1639 (1997).
2. D.-L. Liu and R. C. Waag, Harmonic amplitude distribution in a wideband ultrasonic wavefront after propagation through human abdominal wall and breast specimens, *J. Acoust. Soc. Am.* **101**, 1172 (1997).
3. M. Lou and J. A. Rial, Characterization of geothermal reservoir crack patterns using shear-wave splitting, *Geophysics* **62**, 487 (1997).
4. M. Okoniewski and M. A. Stuchly, A study of the handset antenna and human body interaction, *IEEE Trans. Microwave Theory Tech.* **44**, 1855 (1996).
5. C. Tam and J. Webb, Dispersion-relation-preserving finite difference schemes for computational acoustics, *J. Comput. Phys.* **107**, 262 (1993).
6. C. Pruett, T. Zang, C. Chang, and M. H. Carpenter, Spatial direct numerical simulation of high speed boundary-layer flows, Part I: Algorithmic considerations and validation, *Theoret. Comput. Fluid Dyn.* **7**, 49 (1995).
7. H. O. Kreiss and J. Oliger, Comparison of accurate methods for the integration of hyperbolic equations, *Tellus* **24**, 3 (1972).
8. G. Scherer, On Energy Estimates for Difference Approximations to Hyperbolic Partial Differential Equations, Ph.D. thesis (Dep. Scientific Computing, Uppsala University, 1977).
9. H. O. Kreiss and G. Scherer, Finite element and finite difference methods for hyperbolic partial differential equations, in *Mathematical Aspects of Finite Elements in Partial Differential Equations* (Academic, New York, 1974), p. 195.
10. P. Olsson, High-Order Difference Methods and Data-Parallel Implementation, Ph.D. thesis (Dep. of Scientific Computing, Uppsala University, 1992).
11. B. Strand, High-Order Difference Approximations for Hyperbolic Initial Boundary Value Problems, Ph.D. thesis (Dep. of Scientific Computing, Uppsala University, 1996).
12. B. Strand, Summation by parts for finite difference approximations for d/dx, *J. Comput. Phys.* **110**, 47 (1994).
13. P. Olsson, Summation by parts, projections, and stability I, *Math. Comput.* **64**, 1035 (1995).
14. P. Olsson, Summation by parts, projections, and stability II, *Math. Comput.* **64**, 1473 (1995).
15. M. H. Carpenter, D. Gottlieb, and S. Abarbanel, The stability of numerical boundary treatments for compact high-order finite-difference schemes, *J. Comput. Phys.* **108**, 272 (1994).
16. M. H. Carpenter, D. Gottlieb, and S. Abarbanel, Time-stable boundary conditions for finite-difference schemes solving hyperbolic systems: Methodology and application to high-order compact schemes, *J. Comput. Phys.* **111**, 220 (1994).
17. M. H. Carpenter, J. Nordström, and D. Gottlieb, A stable and conservative interface treatment of arbitrary spatial accuracy, *J. Comput. Phys.* **148**, 341 (1999).
18. J. Nordström and M. H. Carpenter, Boundary and interface conditions for high order finite difference methods applied to the Euler and Navier–Stokes equations, *J. Comput. Phys.* **148**, 621 (1999).
19. D. A. Kopriva, Spectral methods for the Euler equations, the blunt body problem revisited, *AIAA J.* **29**, 1458 (1991).
20. J. S. Hesthaven and D. Gottlieb, A stable penalty method for the compressible Navier–Stokes Equations: 1. Open boundary conditions, *SIAM J. Sci. Comput.* **17**, 579 (1996).
21. J. S. Hesthaven, A stable penalty method for the compressible Navier-Stokes Equations: II. One-dimensional domain decomposition schemes, *SIAM J. Sci. Comput.* **18**, 658 (1997).
22. B. Sjögren, High-order centered difference methods for the compressible Navier–Stokes equations, *J. Comput. Phys.* **117**, 251 (1995).
23. J. Hyman, M. Shashkov, J. Castillo, and S. Steinberg, High order mimetic finite difference methods on nonuniform grids, in *Proceedings from ICOSAHOM 95* (Houston, Texas, 1995), Paper 11.

24. J. S. Hesthaven, A stable penalty method for the compressible Navier–Stokes Equations: III. Multidimensional domain decomposition schemes, *SIAM J. Sci. Comput.* **20**, 62 (1998).
25. B. Gustafsson, H. O. Kreiss, and J. Oliger, Time Dependent Problems and Difference Methods (John Wiley, New York, 1996).
26. C. Van Loan, Computational Frameworks for the Fast Fourier Transform (Soc. for Industr. & Appl. Math. Philadelphia, 1992).
27. J. Nordström and M. H. Carpenter, High Order Finite Difference Methods, Multidimensional Linear Problems and Curvilinear Coordinates, NASA/CR-1999-209834, ICASE Rep. No. 99-54 (Institute for Computer Applications in Science and Enginering MS 132C, NASA Langley Research Center, Hampton, VA 23681-2199, Dec. 1999).
28. J. Nordström, On flux-extrapolation at supersonic outflow boundaries, *Appl. Numer. Math.* **30**, 447 (1999).
29. J. Nordström, The use of characteristic boundary conditions for the Navier–Stokes equations, *Comput. Fluids* **24**, 609 (1995).
30. M. H. Carpenter and C. A. Kennedy, Fourth-Order 2N-Storage Runge–Kutta Schemes, NASA-TM-109111 (Apr. 1994).
31. F. M. White, Viscous Fluid Flow (McGraw-Hill, New York, 1974).
32. B. Gustafsson, The convergence rate for difference approximations to mixed initial boundary value problems, *Math. Comput.* **29**, 396 (1975).
33. B. Gustafsson, The convergence rate for difference approximations to general mixed initial boundary value problems, *SIAM J. Numer. Anal.* **18**, 179 (1981).